EN/MME
Laboratoire de Mesures Mécaniques / *Mechanical Measurement lab*
Rapport expérimental / *Investigation report*

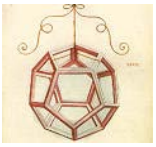

Author: *A.KUZMIN*	*Date:* *07-12-2009*	*EDMS Nr :* *1027459*	*Approved by :* *M.GUINCHARD*
Customer: *Alain Herve*	*Distribution list:* *C. Hauviller - CERN, K. Artoos - CERN, C.Collette – CERN, R.Folch-CERN, O. Capatina – CERN, M. Sylte-CERN; A. Ball – CERN; H. Schmickler - CERN; J.-P. Delahaye – CERN; D. Schulte- CERN.*		

Ground vibration measurements and Experiment parts motion measurement at CMS

1. Abstract.

The ground vibrations, as well as experiment parts motion has been measured at CMS to characterize the ground motion behaviour and to understand the behaviour of future experiments to be installed on CLIC or ILC,.

This report contains the results of the vibration measurements and the noise determinations carried out by the mechanical measurement lab of the EN/ MME group at several places inside the CMS experimental hall.

2. Goals of the measurement.

After discussion with the requestor of these measurements, the following goals were identified:

- Measure the ground motion of the CMS Cavern to complete the knowledge database of the CLIC and ILC stabilization activities.
- Measure the coherence length in an experimental cavern and compare with the previous measurements in the LHC tunnel.
- Evaluate the dynamical behaviour of the YB0, YB1, HF Tower and the concrete slab of the pit.
- Measure the motion of CMS rotating shielding to model the dynamical behaviour of ILC or CLIC final focus quadrupole.

3. Methods and Experimental data.

The measurements were recorded between the 7th September and the 25th September 2009 when the cooling system was off.

3.1. Sensors

The geophones have a differential sensitivity of about 2000 V/(m/s) and a frequency range between 1/30 Hz and 100 Hz. Details concerning the sensor sensitivity are described in attachment 1.
Geophones were adjusted to have the vertical direction parallel to the gravitation force. Longitudinal North-South direction for geophones was pointed in the beam direction towards the Point 4 (North).
The results obtained from these sensors are dependent on good operational conditions and give a good signal to noise ratio only if all conditions are correct. The geophones need to be well protected against fluctuation in temperature and turbulent airflow (2).
In order to have a constant temperature for the geophones during operation they were located and switched on at least half an hour before any measurement was started. Then they had time to reach thermodynamic equilibrium, which provide a minimum of temperature fluctuation. To turn on

the geophones some hours before measurement also remove a DC offset, which give a possibility to reduce the dynamic range and therefore give a better accuracy.

3.2. Acquisition system

The acquisition system used was the MKII made by Müller-BBM. The MKII system is a real time spectrum analyzer and compact data acquisition system. It contains 16 input channels with DSP (Digital Spectral Processing) for each channel with a sampling frequency up to 384 kHz. The dynamic resolution is 24bits, and can be used on a range between 10mV and 50V.
The system is controlled by PAK Software, measuring, analyzing and interpreting recorded signals. PAK software allows analysis such as FFT (Fast Fourier Transform), PDS (Power Spectral Density) and CPS (Cross Power spectrum) to be carried out. Excel was used to calculate the RMS Integrated and the noise levels.

PAK MÜLLER-BBM Version:MKII

Figure 1. Spectrum analyzer.

Figure 2. Geophones.

3.3. Signal treatment.

Power Spectrum

The Power Spectrum of a signal is the average of the square magnitude of a number of instantaneous spectra. Since the square of an imaginary part is real, this spectrum has only a real part (4). The calculation of the power spectrum is showed in Equation 1.

$$G_{aa} = \overline{(S_a \times S_a)}$$

Equation 1

Since in most applications it is more interesting to observe the linear units, the square root of the power spectrum is commonly displayed.

$$\text{RMS Spectrum} = \sqrt{G_{aa}}$$

Equation 2

The RMS spectrum is the square the Power Spectrum and is therefore also real.

Power Spectral Density

The PSD (Power Spectral Density) of a signal is the Power Spectrum divided by the bandwidth of each frequency and has the unit x^2/Hz. The PSD show how the power of the signal is distributed versus the frequency (4).

$$\Phi = \frac{G_{aa}}{Bandwith}$$

Equation 3

The purpose of the PSD is to give an understanding of the wideband noise, for instance white noise. Since white noise has a uniform energy distribution across all frequencies, the signal would be read with just half the energy after halving the filter bin. One way around this problem is to define the amplitude using the PSD.
This returns that for a single frequency normal amplitude readings should be used, but for wideband noise such as white noise, PSD should be used.

There is a confusion concerning PSD that has to be taken into consideration. Suppose that a period of white noise is measured and Hanning windowed. At the beginning and at the end of the period, the noise will be reduced by effect of the Hanning window; the result will be less energy in the signal than there actually is. For a Hanning window the correct value can be obtained by multiplying the result by a correction factor of 2/3.

Average Cross Spectrum

The average cross spectrum is the most important dual channel function, even though it by itself has no function, it is however used to calculate every other dual channel functions.
The average cross spectrum is the vector product of the spectra of two signals (4), and is calculated in Equation 4.

$$G_{ab} = \overline{(S_b \times S_a^*)} = real + j \times imaginary$$

Equation 4

S_a^* is the complex conjugate of S_a

RMS Integrated

RMS Integrated is used to sum up the total vibration in a spectrum. As the name indicates it gives the RMS (Root Mean Square) value of the total vibration. The RMS Integrated is given by Equation 5.

$$RMS_{\text{int}}(k) = \sqrt{\sum_{k1}^{k2} PSD(k) \times \Delta f}$$

Equation 5

RMS Integrated is a function of k, the frequency. It is usual to plot the RMS Integrated as a graph where you use k_2 as a fixed upper value and gradually reduce k_1 while you plot the RMS Integrated for each value of k_1. Then it is possible to see the total summation of vibrations from a frequency and down to every lower frequency. In this report, 100 Hz is used for the value of k_2 and 0.01 Hz for
k_1.

The method used to calibrate the RMS Integrated in this report has been thoroughly validated using two different programs.

4. Results.

4.1. Ground motion.

To determine the ground vibration level in CMS cavern, two geophones were placed close together on the floor under YB0 barrel.
The graph shown below represents RMS integrated in all three directions and the noise level.

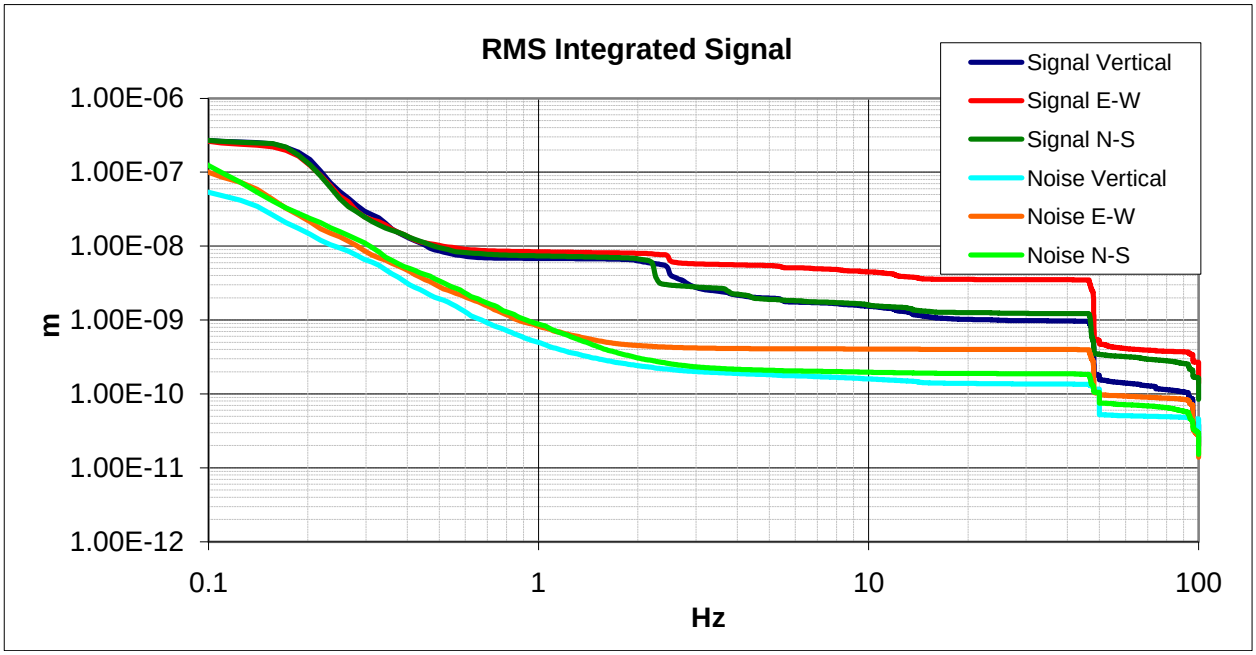

Figure 3. RMS Integrated. Ground motion.

Comparing ground vibration level in LHC tunnel and in CMS cavern it could be seen that the level at CMS experiment is notably higher by almost factor 10. The measurements in CMS cavern were performed during the day while experiment maintenance. Important thing is that the cooling system was off during the measurements. So, much higher level of vibrations has to be expected when the cooling system will be running but it is difficult to evaluate the impact on the RMS integrated value.
In order to validate the measurements, the signal to noise ratio of the sensors was calculated and plotted in attachment B : these measurements can be considered as valid in the signal to noise ratio point of view.
Additional graphs can be found in the attachment B.

4.2. YB0 barrel motion.

To determine the motion of fixed barrel YB0, two geophones were placed as shown on the following picture. The reference geophone was placed on the floor under the barrel and other geophone was on the top of it.

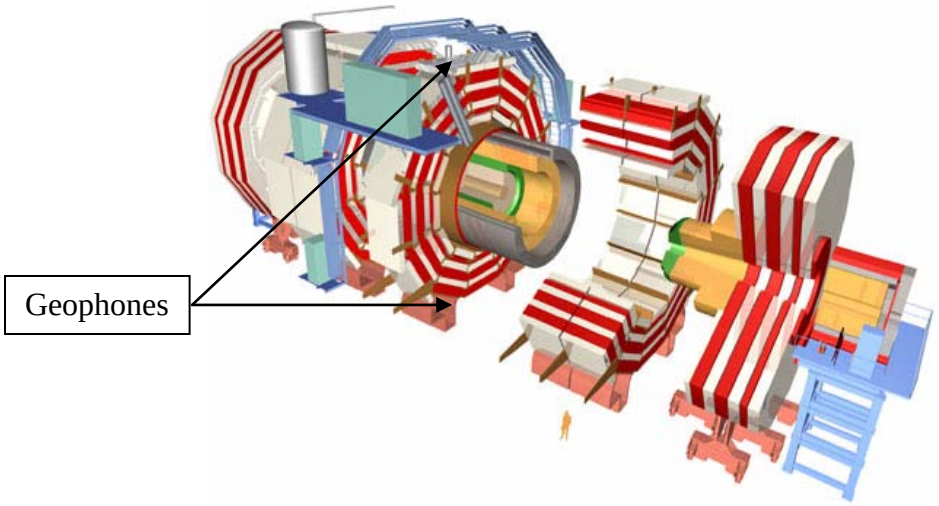

Figure 4. YB0 motion measurement.

The graphs containing the PSD (Power Spectrum Density) for all three directions (Vertical, North-South and East-West) are shown in attachment C
The RMS integrated for both signals (geophone placed on the ground and geophone placed on the top of the barrel) in all three directions is shown on Figure 5.

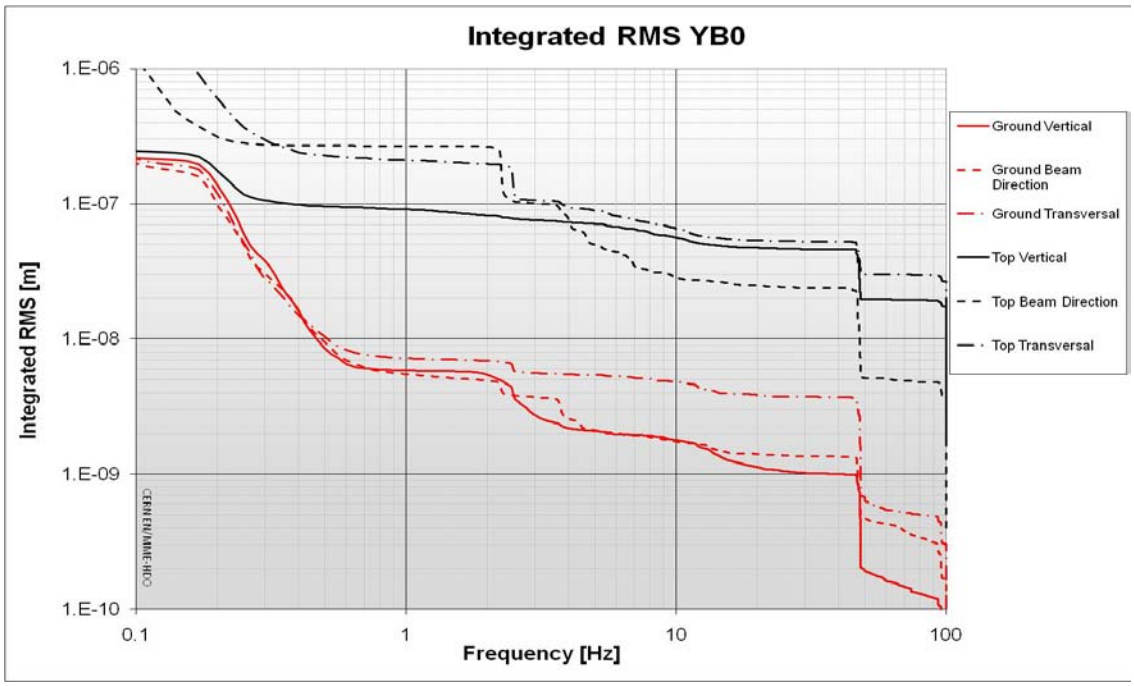

Figure 5. RMS Integrated YB0.

The transfer function between two geophones was calculated and is plotted in the attachment C for all three directions. These curves allow identifying amplifications at several frequencies (2.2Hz, 4 Hz, etc...) mainly in the beam direction but do not permit to assume that these frequencies correspond to the natural frequencies of the YB0 barrel (No phase shift and no correlation with the coherence curves).

4.3. YB1 barrel motion.

The motion of mobile barrel YB1 was measured in similar way as YB0 i.e. reference geophone was kept under YB0 to have the same reference for both measurements and the other geophone was placed on the top of YB1 barrel.
The PSD graphs are shown in attachment D. The RMS integrated was calculated for both signals and plotted below.

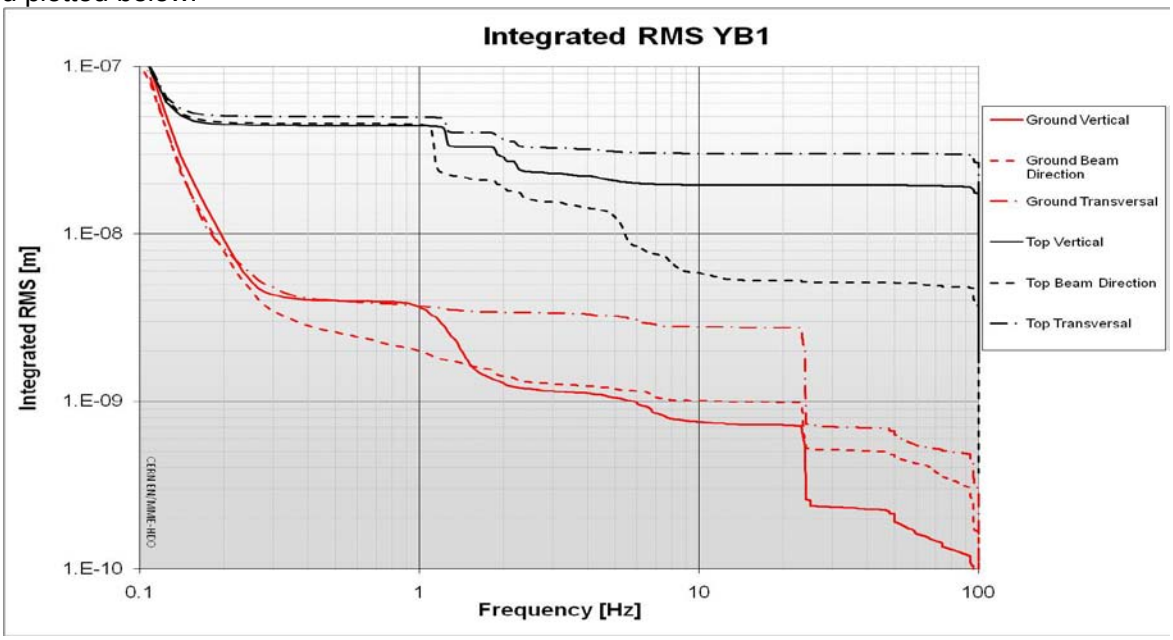

Figure 6. RMS Integrated YB1

Comparing RMS integrated for YB0 and YB1 it could be seen that the motion level of YB1 is lower than the one of YB0. Note that the ground vibration level was also lower during YB1 measurement. This difference can be explained by the fact that the measurements were taken one after another during the day while the maintenance of the machine was in progress.

4.4. HF Tower motion.

To determine the motion of HF structure, two geophones were placed as shown on the following picture. The reference geophone was placed on the floor under HF structure and other geophone was on the top of it.

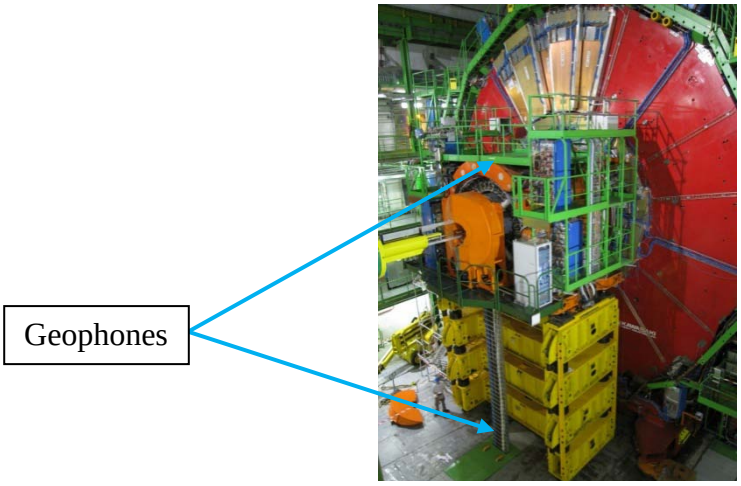

Figure 7. HF Tower motion measurement.

The PSD curves are in attachment E and RMS Integrated is shown below.

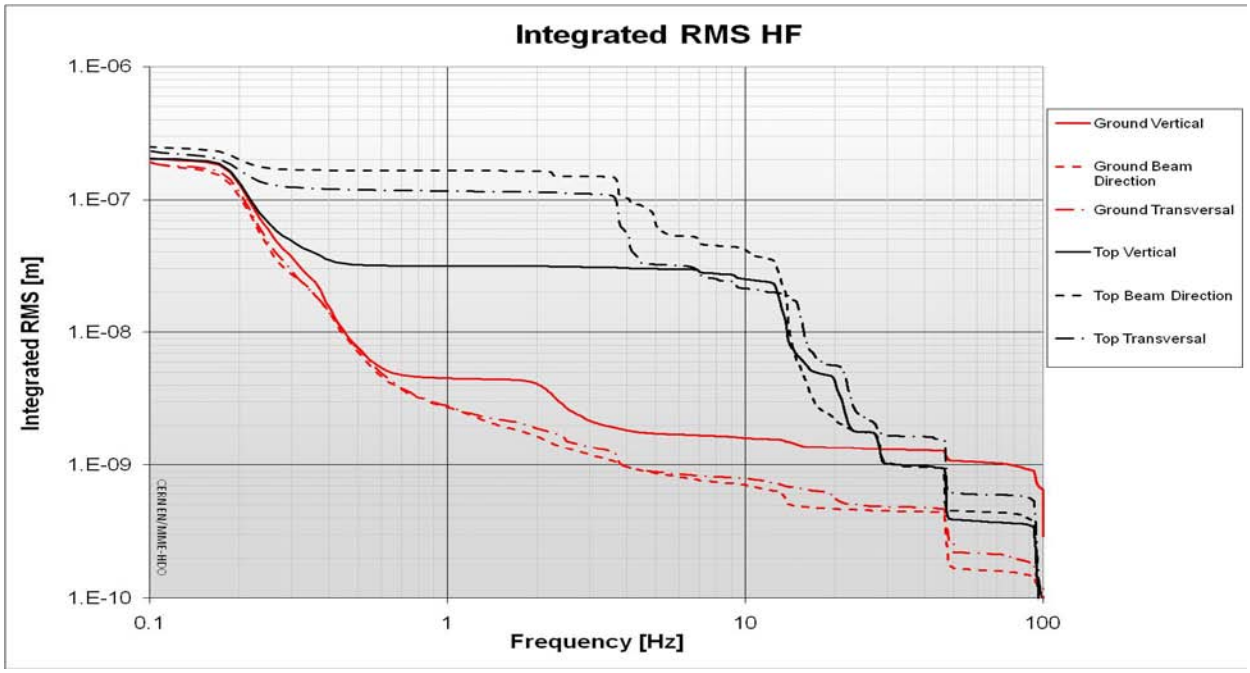

Figure 8. RMS Integrated HF Tower.

4.5. Rotating Shielding motion.

One extremity of the rotating shielding is attached to the wall but the second one can be considered as free.
To determine the motion of shielding, two geophones were placed as shown on the picture below. The reference geophone was placed close to the wall and other geophone was on the extremity of the shielding (Figure 9).

Figure 9. Rotating Shielding Motion Measurement.

Throughput signal from geophones in vertical direction is shown on Figure 10. This graph shows that the free extremity seems to be excited by a frequency 4.9Hz. This frequency can be a natural frequency of the rotating shielding or an external excitation delivered from the experiment via the fixed part of the shielding or the connection to the detector.

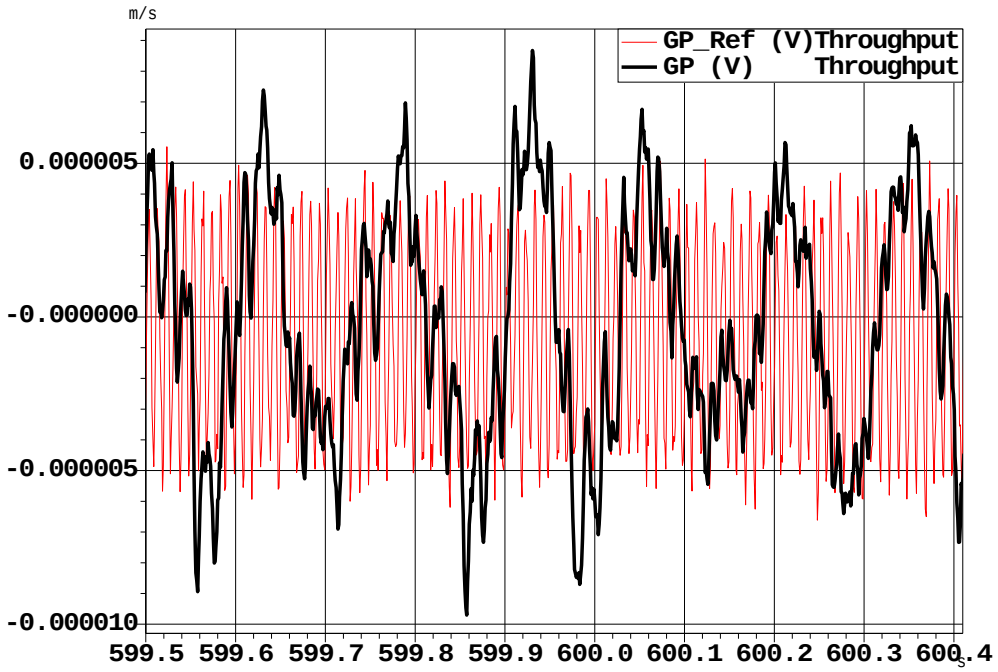

Figure 10. Throughput data. Vertical direction.

The PSD curves for both signals in three directions are plotted in attachment F. The RMS integrated graph and transfer function in the vertical direction between two geophones are plotted below.

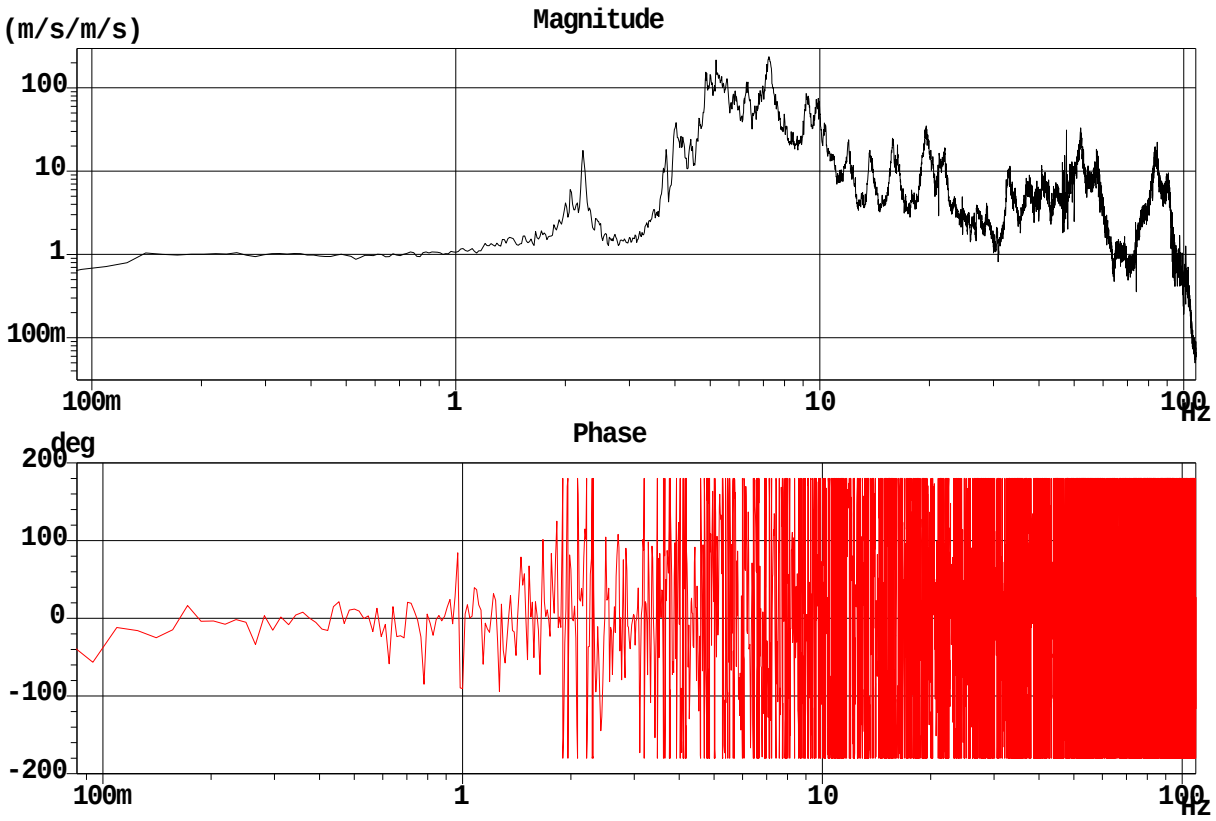

Figure 11. Transfer function in the vertical direction.

The graph shows that the rotating shielding is excited by one frequency at 2.2Hz. The phase diagram does not permit to conclude that this frequency is a natural frequency of the system.

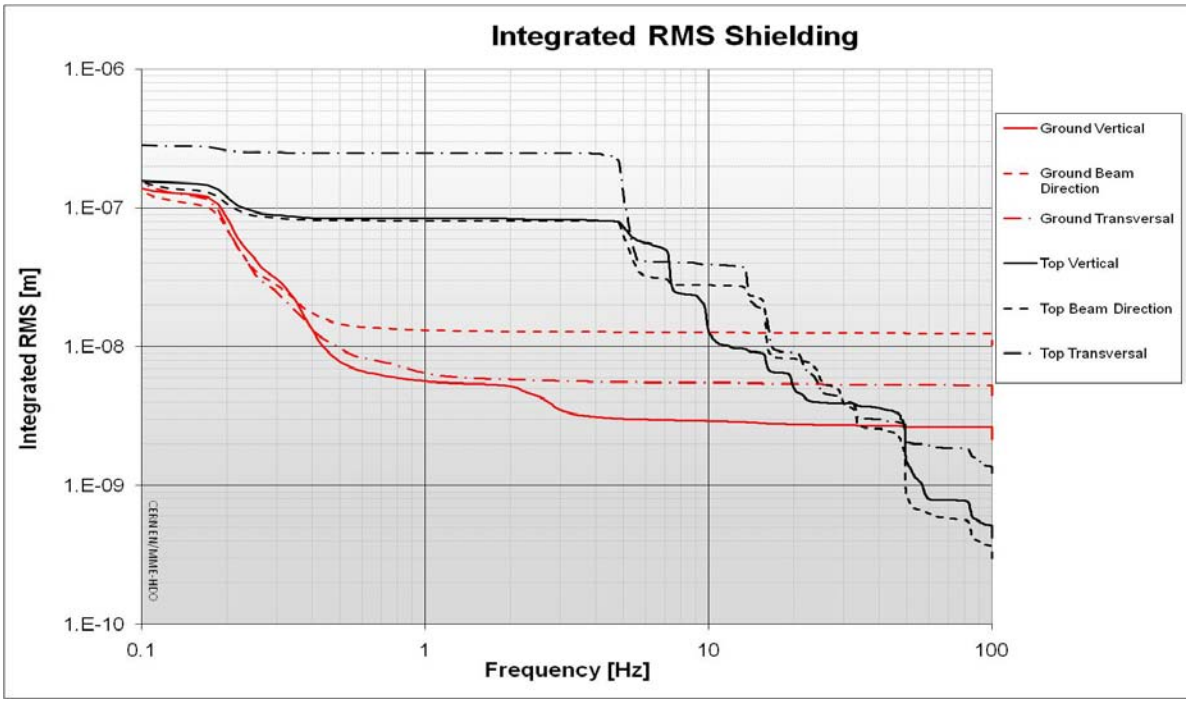

Figure 12. RMS Integrated Rotating Shielding.

4.6. Coherence length measurement.

The coherence of ground motion in the CMS cavern was measured by two geophones placed at different distance from each other. Three measurements were provided:

- Geophones put side by side under YB0

- Reference geophone remains on the same position but the other one has been moved 2.5 meters away along the beam direction.
- Reference geophone on the same position but the other one has been moved along the beam direction 4.8 meters away.

The coherence functions are plotted below

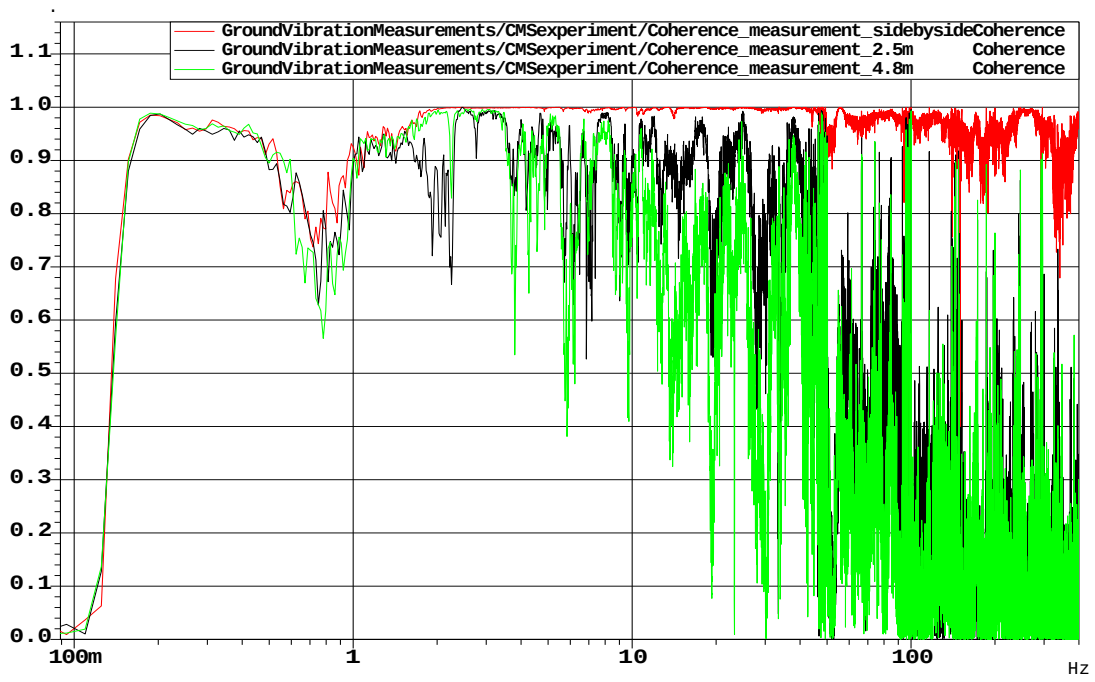

Figure 13. Coherence.

It could be seen on the plot that the coherence decreases after some meters at frequencies above 1 Hertz. These curves have to be compared to the coherence measurements performed in the LHC tunnel in 2008.

4.7. Slab motion measurements.

Two measurements of the motions of the massive slab covering the CMS shaft were done. For the first measurement, the reference geophone was placed on the slab just above the rail and the measuring geophone was placed on the middle of the slab. The transfer function calculated as ratio of Average Power Spectrum of the signals is shown below.

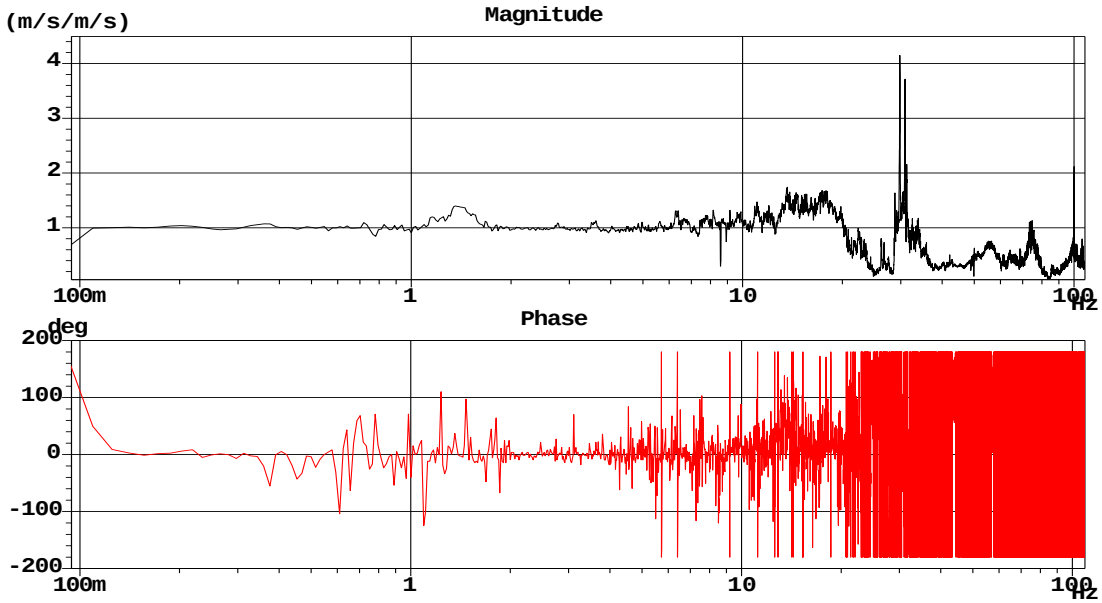

Figure 14. Transfer function in the vertical direction. Reference geophone is above the rail.

The second measurement was taken with the reference geophone moved to the fixed part (floor of CMS hall)

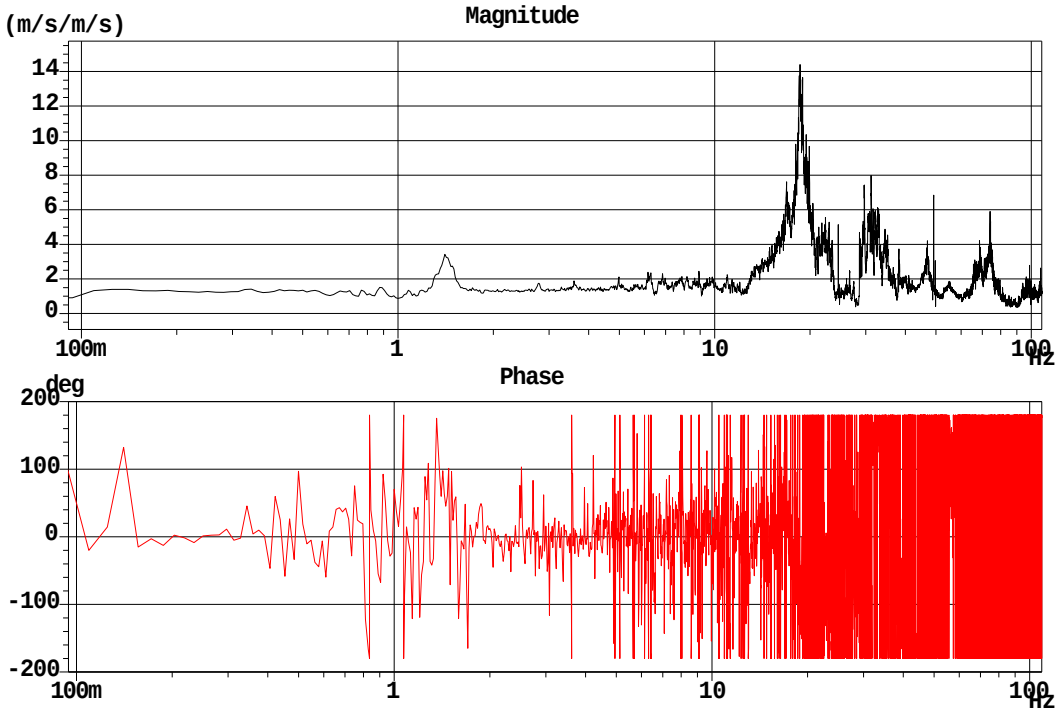

Figure 15. Transfer function in the vertical direction. Reference geophone on the floor.

The RMS Integrated for this measurement is plotted in Figure 16.

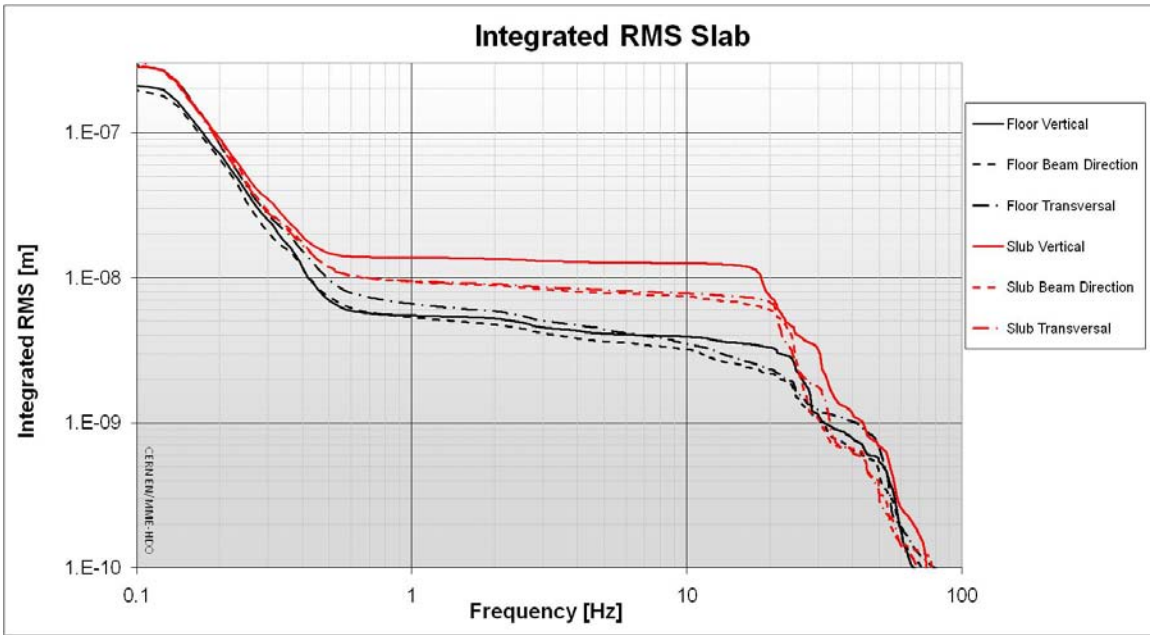

Figure 16. Integrated RMS Slab.

5. Conclusions

- The table below summarizes the measurements of different experiment parts :

		RMS Integrated for vertical direction		First frequency excited		
		1 Hz	10 Hz	Vertical	North-South	East-West
YB0	Top	91 nm	56 nm	2.2Hz	2.2Hz	2.5Hz
	Ground	6 nm	2 nm			
YB1	Top	44 nm	20 nm	2.2Hz	2.2Hz	2.5Hz
	Ground	4 nm	0.8 nm			
HF Tower	Top	31 nm	25 nm	2.2Hz	2.2Hz	2.5Hz
	Ground	5 nm	1.6 nm			
Rotating Shielding	Fixed Extremity	84 nm	13 nm	2.2Hz	2.2Hz	2.5Hz
	Free Extremity	6 nm	3 nm			
Slab	Floor	5 nm	4 nm	-	-	-
	Slab	13 nm	13 nm	1.4Hz	-	-

- The coherence in CMS cavern decreases slowly in comparison with the one in the LHC tunnel (5). This phenomenon can be explained by two facts: joints between concrete modules of the floor in the LHC and a solid floor in CMS; the presence of 12500 tonnes detector on the floor of CMS cavern.

- The RMS integrated levels shown above were calculated for the measurements provided while the cooling system was off. Higher levels have to be expected when the cooling system will be running.

- All these results show that all the experiment parts of CMS cavern are excited at several frequencies. These frequencies could be explained by the natural frequencies of the barrels or by external excitation. The first explanation is that the motion due to the natural frequencies of the most massive part of the experiment (YB0) is distributed over the whole experiment through the floor, walls and mechanical connections between parts. The second explanation could be an external excitation provided by one or a combination of many systems like pumps, compressors or other services.
  To have more precise results, more measurements like modal measurements has to be provided. Computation of the dynamic behaviour would be also useful to understand the origin of the measured frequencies.

6. References

1. **Artoos, K, et al.** *Ground vibration and coherence lenght measurements for the CLIC Nano-Stabilization studies.* 2009.
2. **Systems, Guralp.** *Creating low noise* enviroments for surface seismometers. 2009..
3. **M. Sylte.** *Ground Vibration Measurements at CERN in 2009.*
4. **Montag, Christoph.** *Active stabilization of mechanical quadrupole vibrations for linear colliders.* Germany : s.n., 1996.
5. **M. Sylte**. Effects of the concrete joints on the vibration coherence in the LHC tunnel

8. Attachments

A. Acquisition and analysis parameters:

Geophones GURALP CMG-6T
Link: (http://www.guralp.com/)

	SN T6946	SN T6945
Vertical	2 x 998 V/(m/s)	2 x 996
North/South	2 x 998 V/(m/s)	2 x 1016
East/West	2 x 1003 V/(m/s)	2 x 991

Acquisition and Analysis Parameters:
Sampling Rate: 1024 Hz
Measurement length: 1108s
Block duration: 64s
Overlap: 66.7%
Window: Hanning
Averaging: Linear

B. Ground motion measurements:

Graphs shown below contain:

- the PSD (Power Spectrum Density)
- RMS Integrated signal for both geophones and the noise level
- signal to noise ratio

These graphs are plotted for all three directions (Vertical, North-South and East-West). APSD x-channel/RMS_PSDx and APSD y-channel/RMS_PSDy represent the two signals and Noise Power Spectrum/RMS_noise represent the noise level.

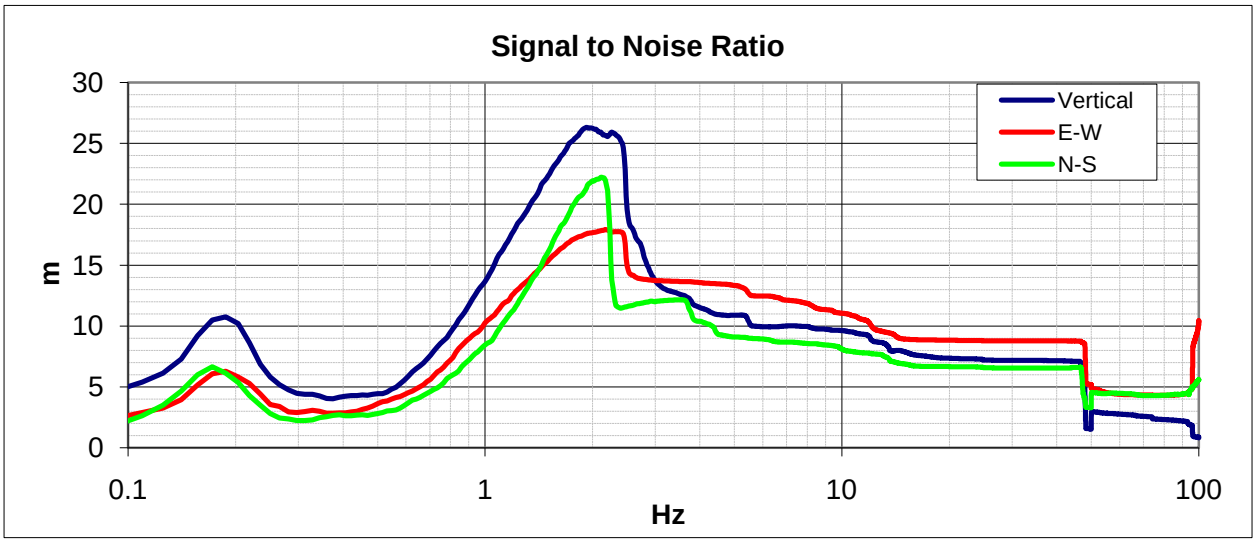

Figure B1. Signal to noise ratio.

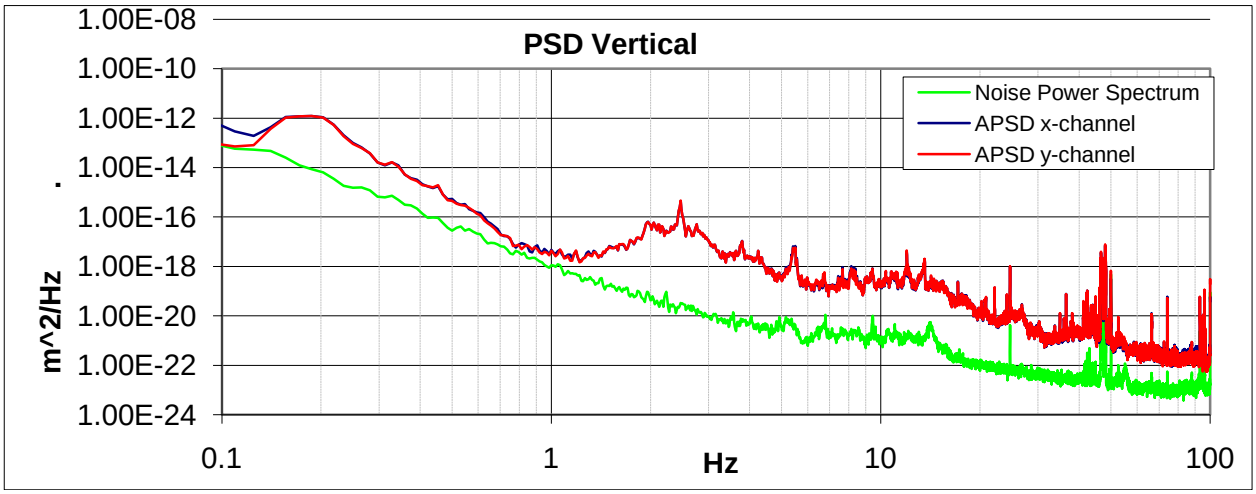

Figure B2

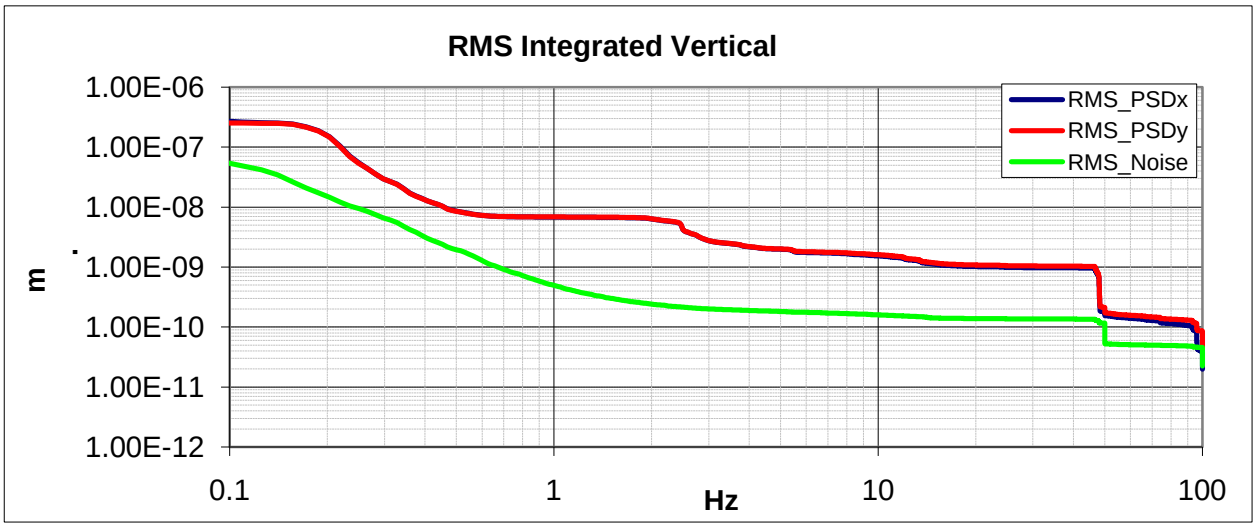

Figure B3

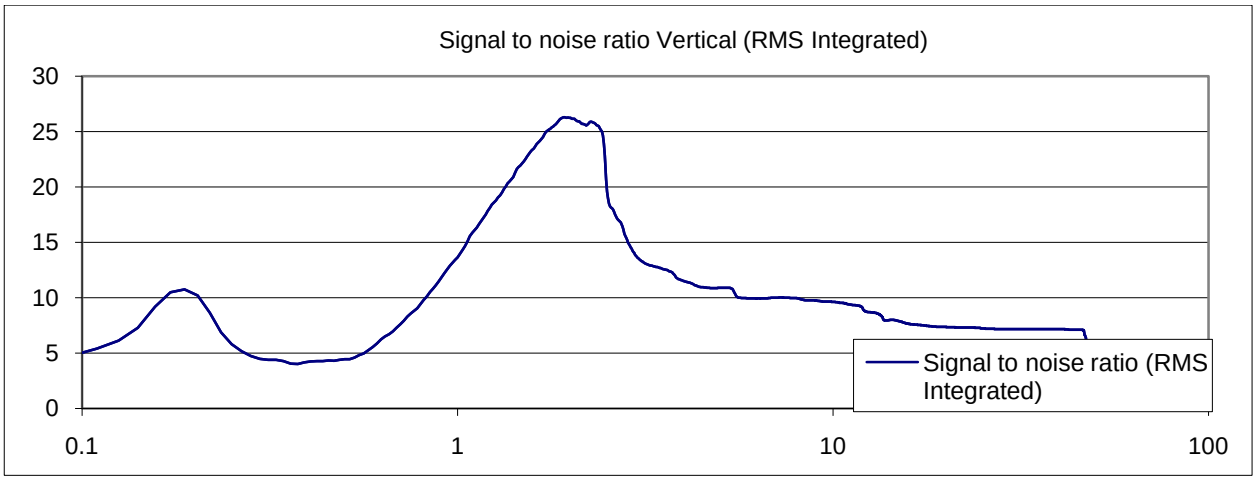

Figure B4

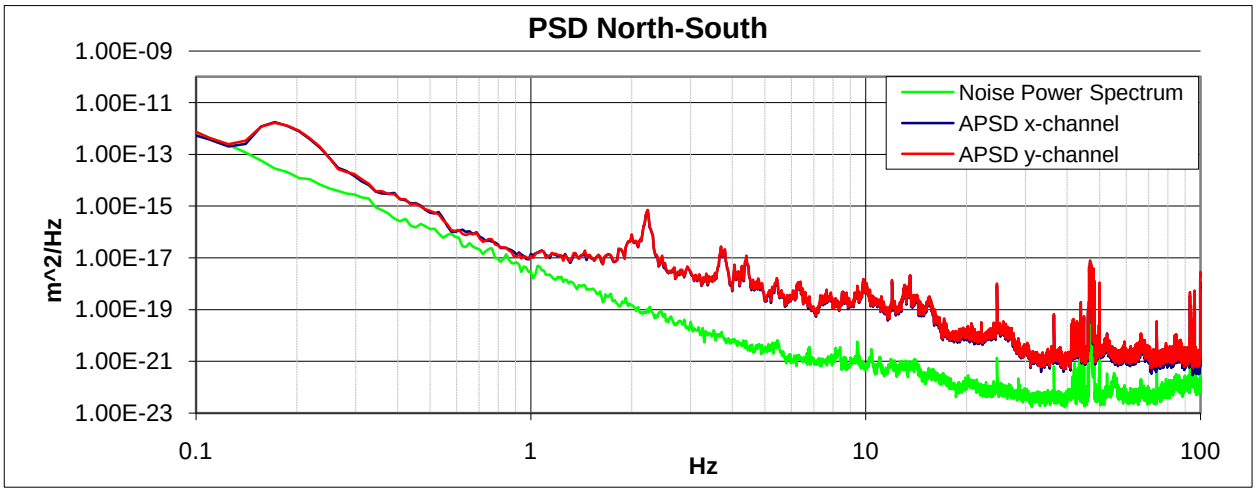

Figure B5

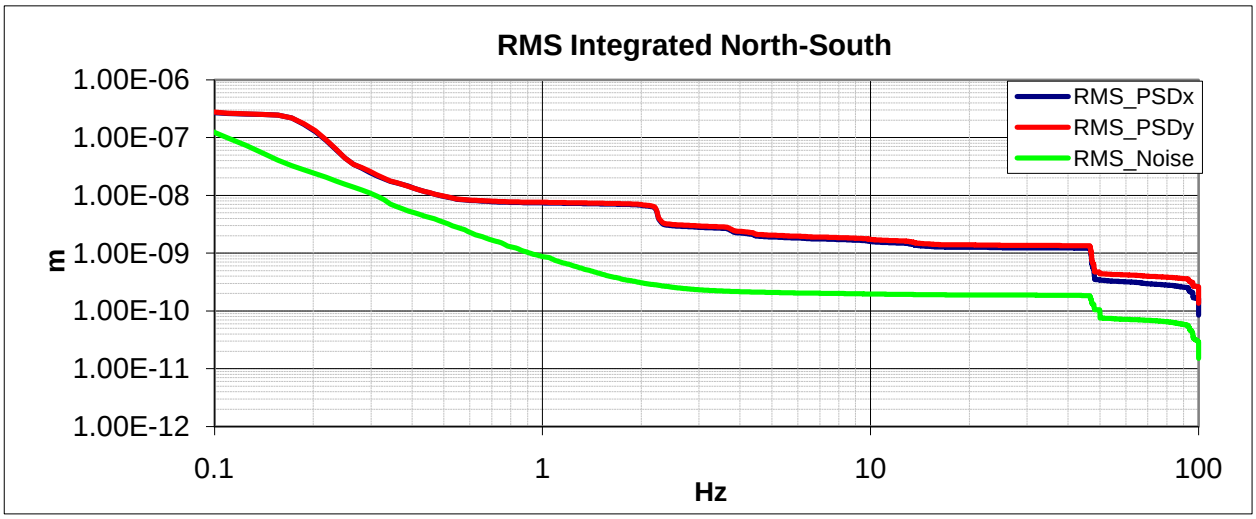

Figure B6

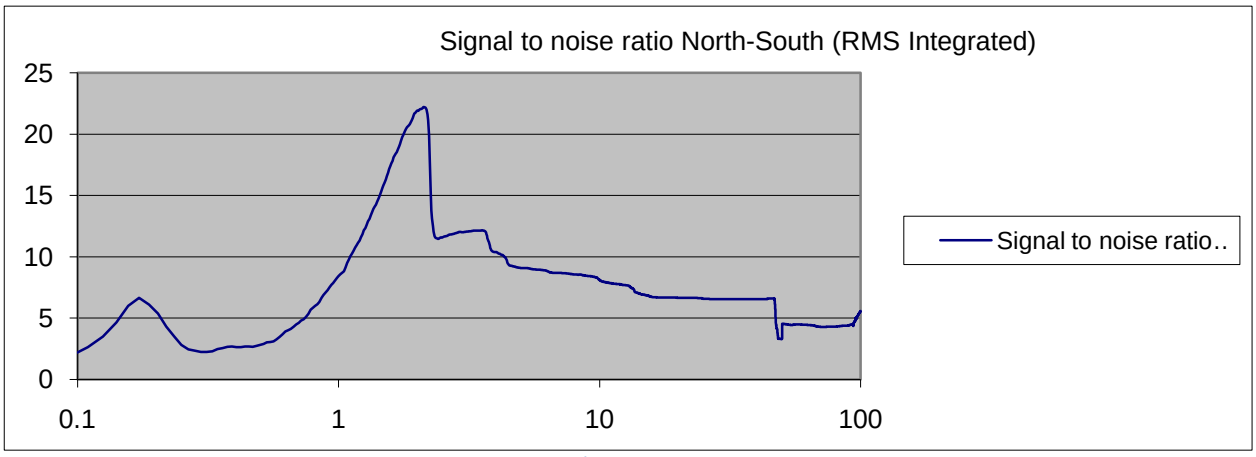

Figure B7

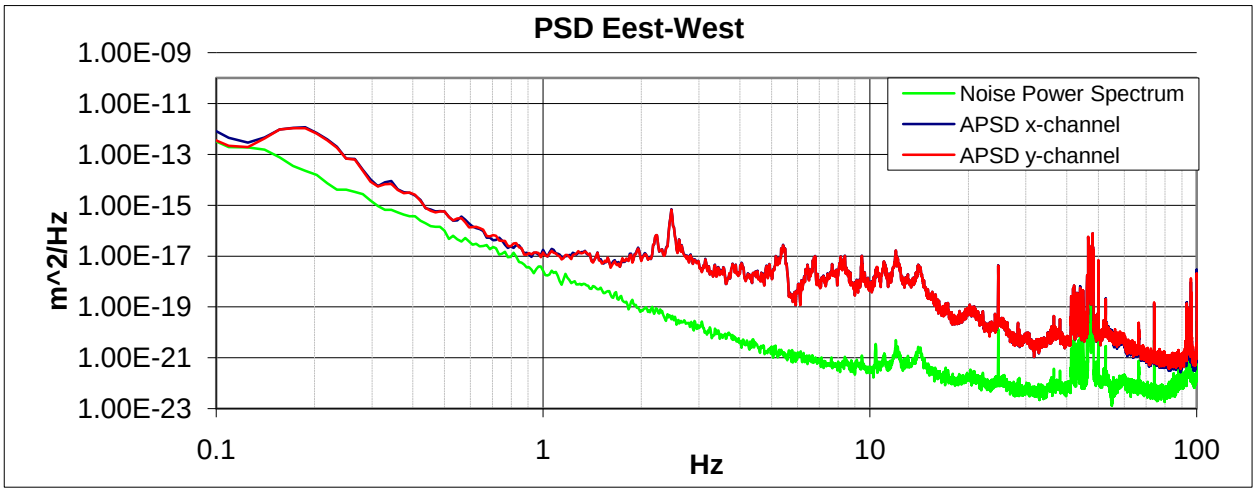

Figure B8

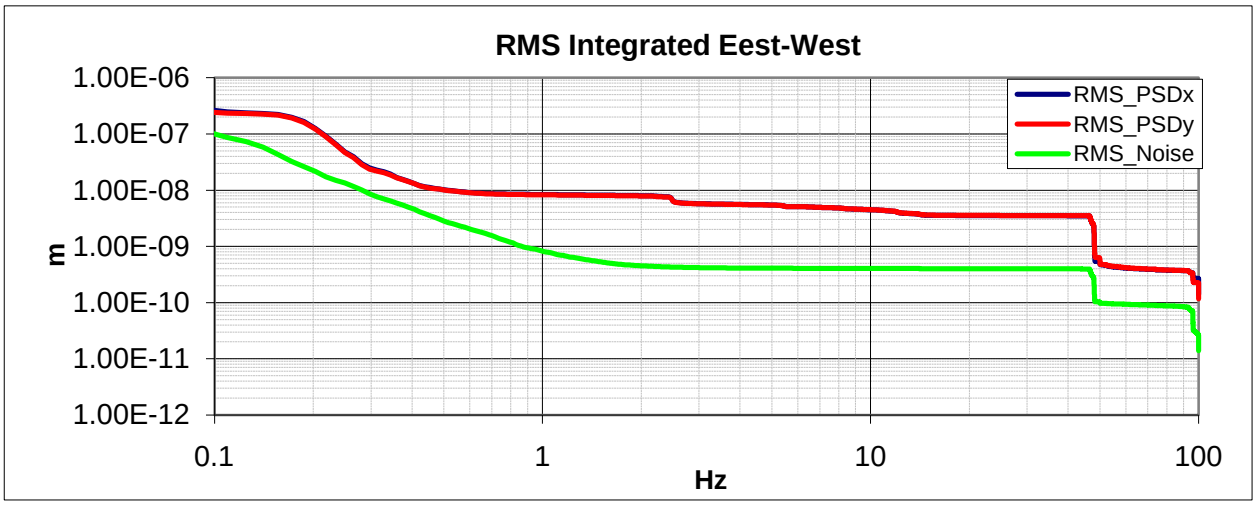

Figure B9

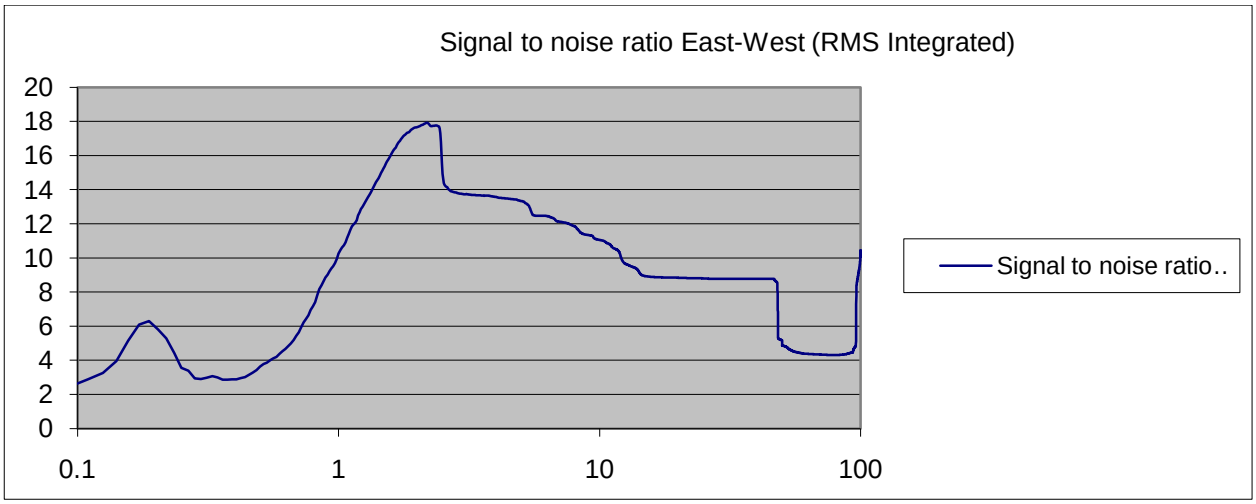

Figure B10

C. *YB0 motion measurement.*

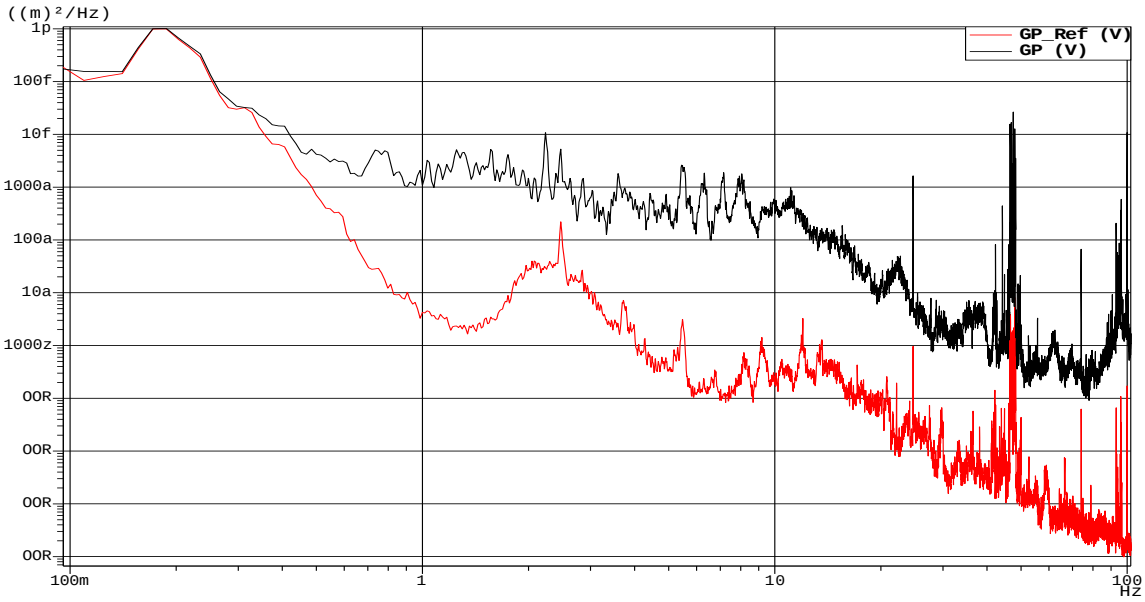

Figure C1. PSD of the signal Vertical direction.

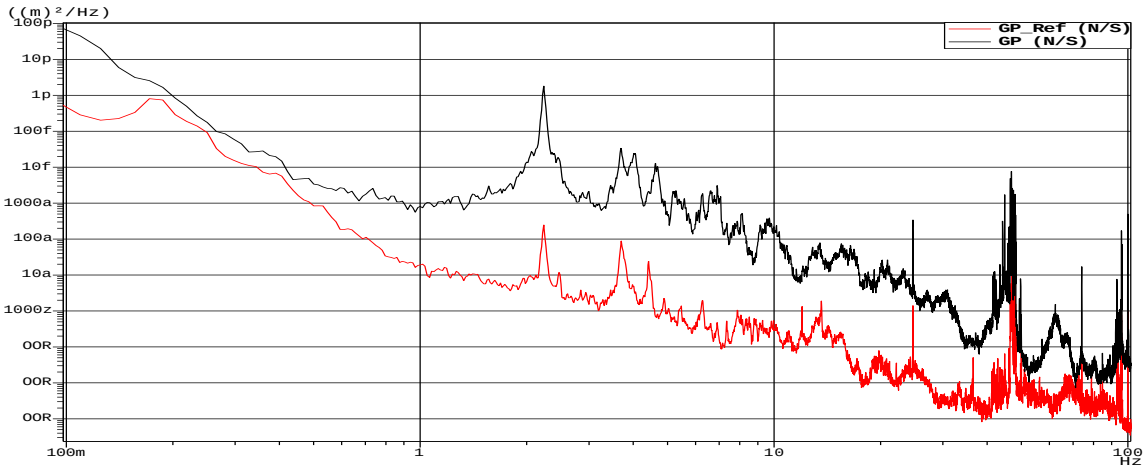

Figure C2. PSD of the signal North-South (Beam) direction.

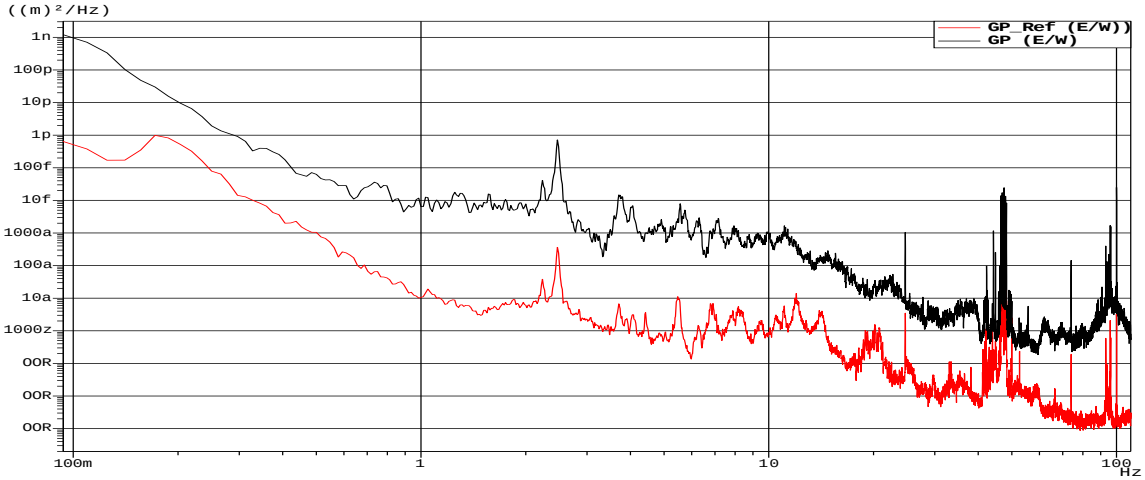

Figure C3. PSD of the signal East-West (Transversal) direction.

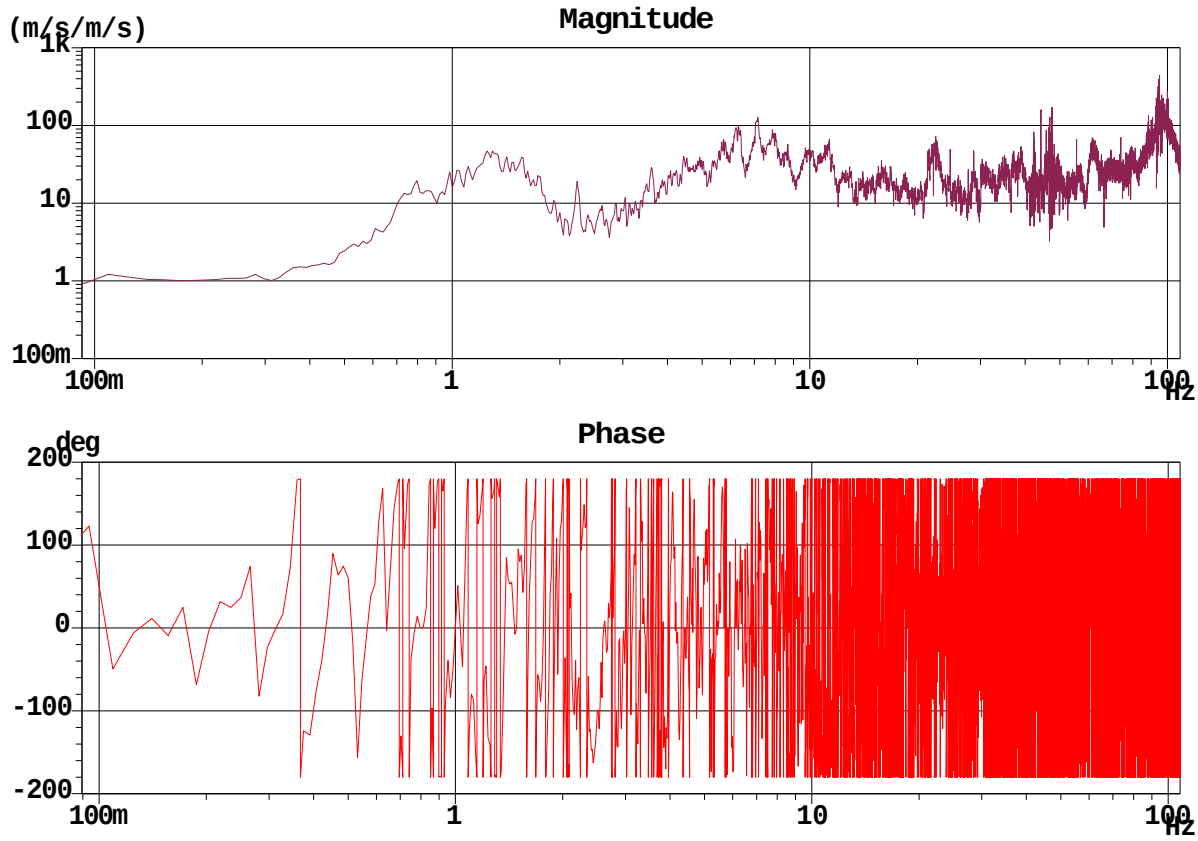

Figure C4. Transfer function YB0 in the vertical direction

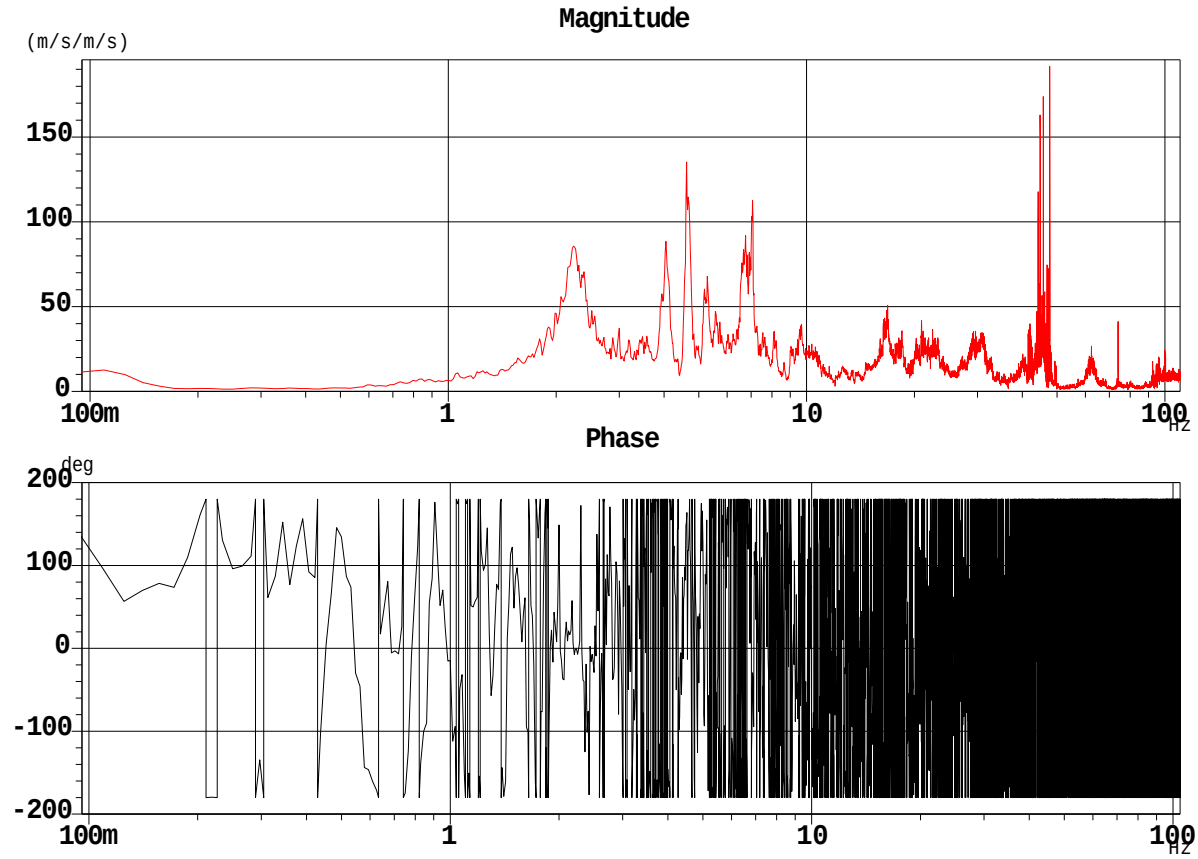

Figure C5 : Transfer Function YB0 in the beam direction

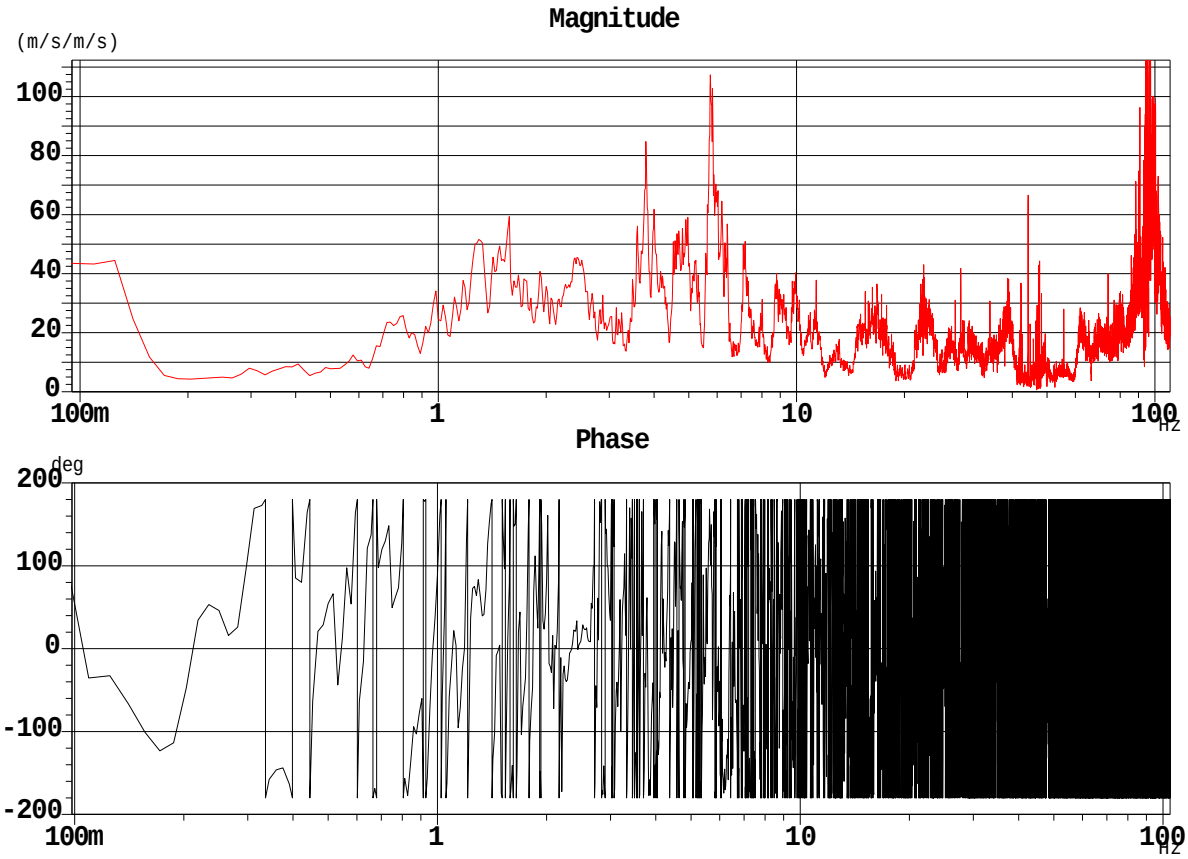

Figure C6 : Transfer function YB0 in the E-W direction

D. YB1 motion measurement.

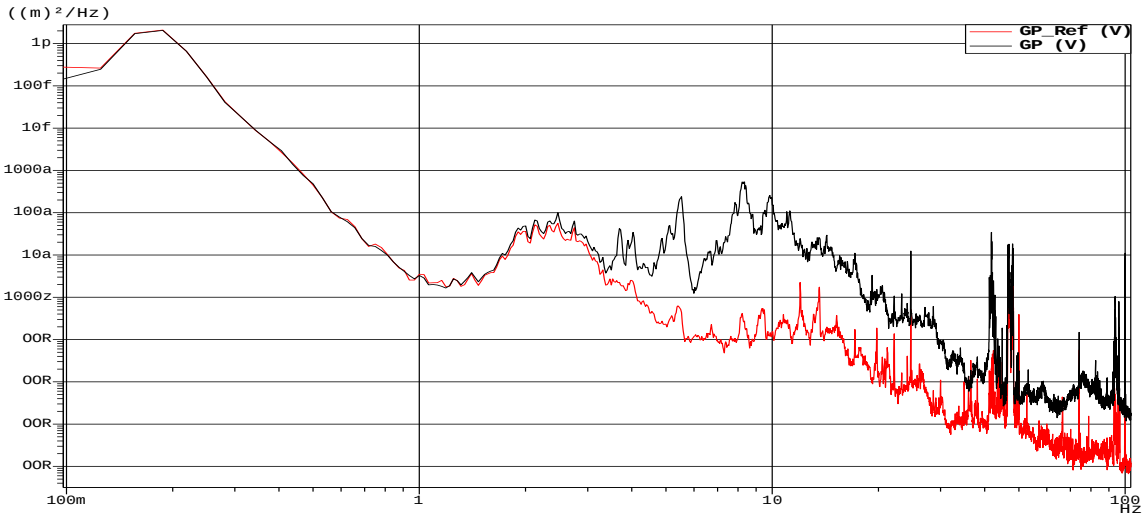

Figure D1. PSD of the signal Vertical direction.

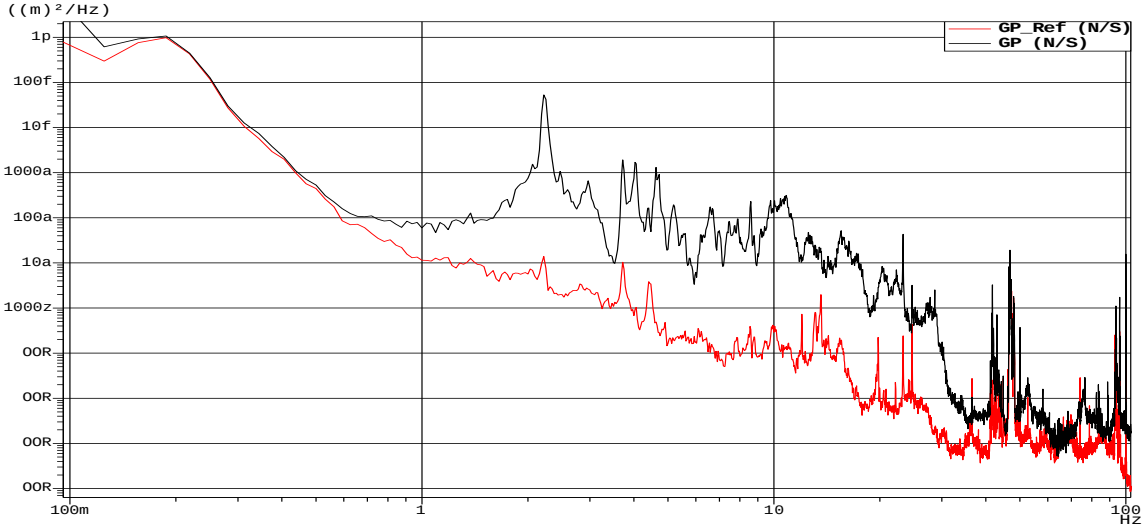

Figure D2. PSD of the signal North-South (Beam) direction.

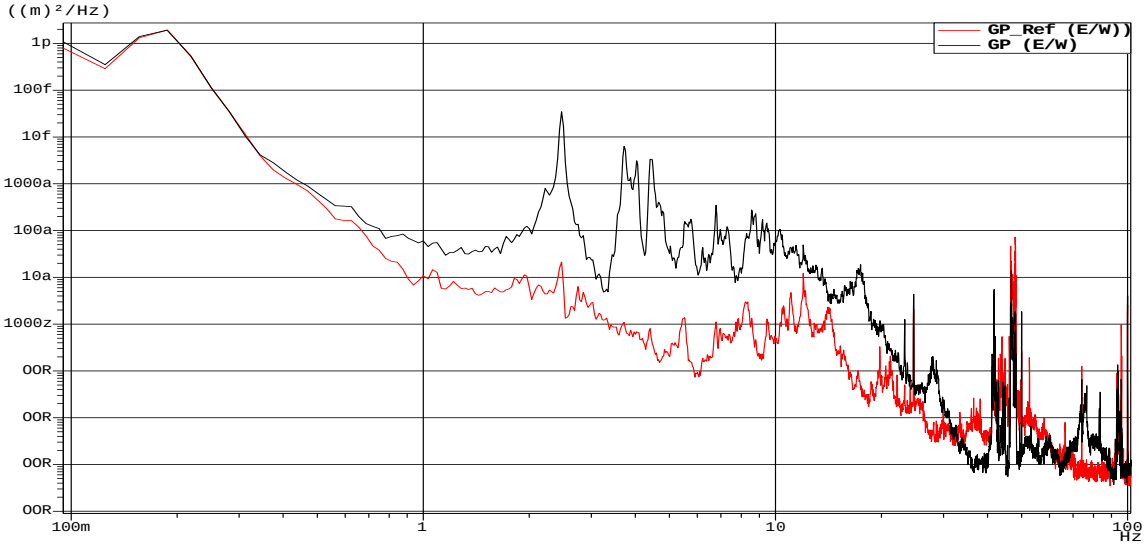

Figure D3. PSD of the signal East-West (Transversal) direction.

E. HF Tower motion measurement.

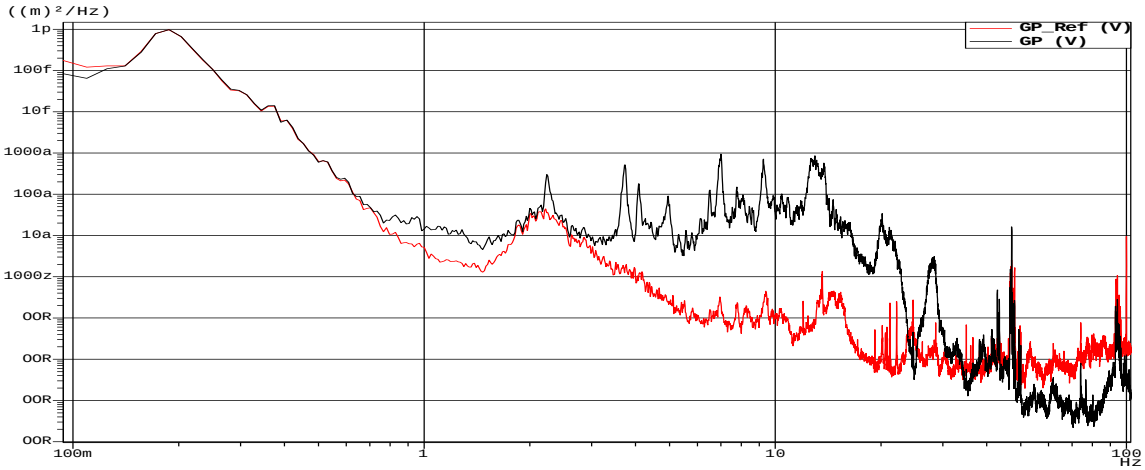

Figure E1. PSD of the signal Vertical direction.

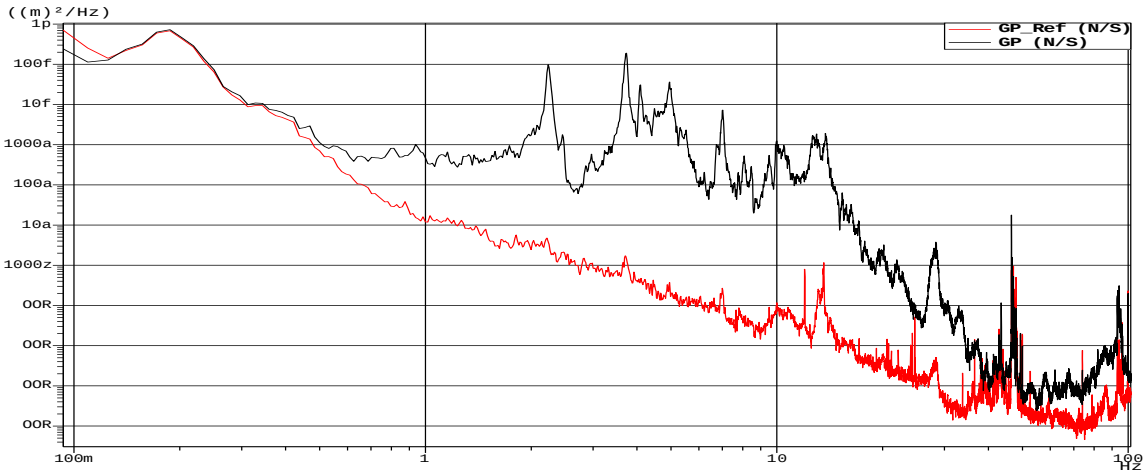

Figure E2. PSD of the signal North-South (Beam) direction.

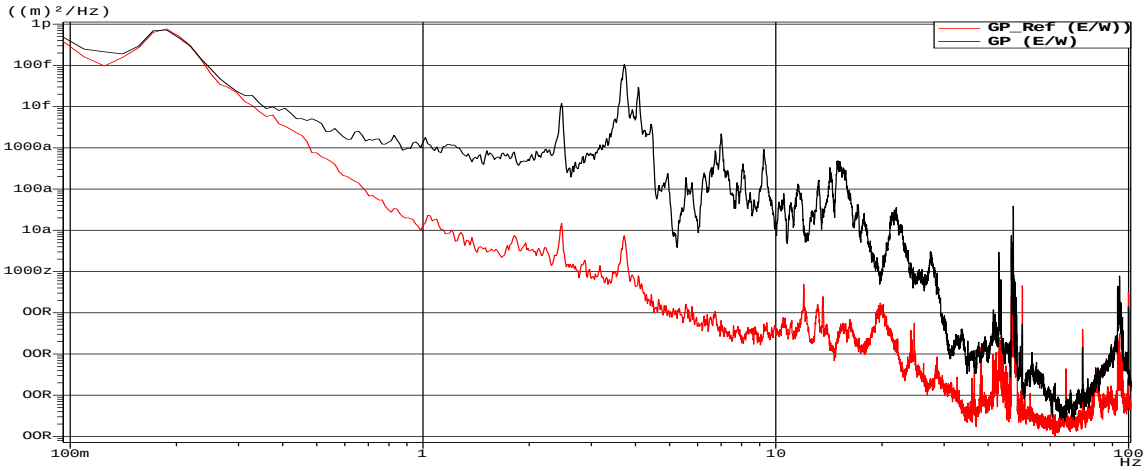

Figure E3. PSD of the signal East-West (Transversal) direction.

F. Rotating Shielding motion measurement.

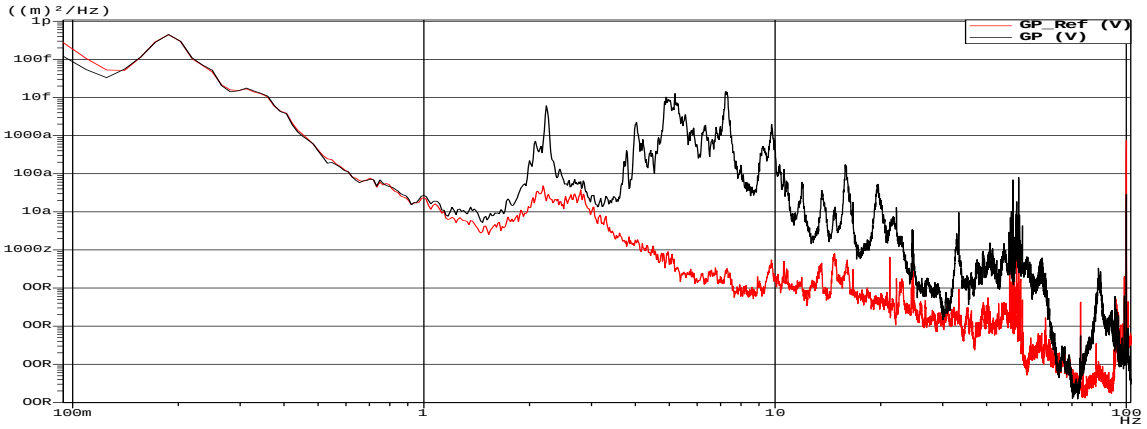

Figure F1. PSD of the signal Vertical direction.

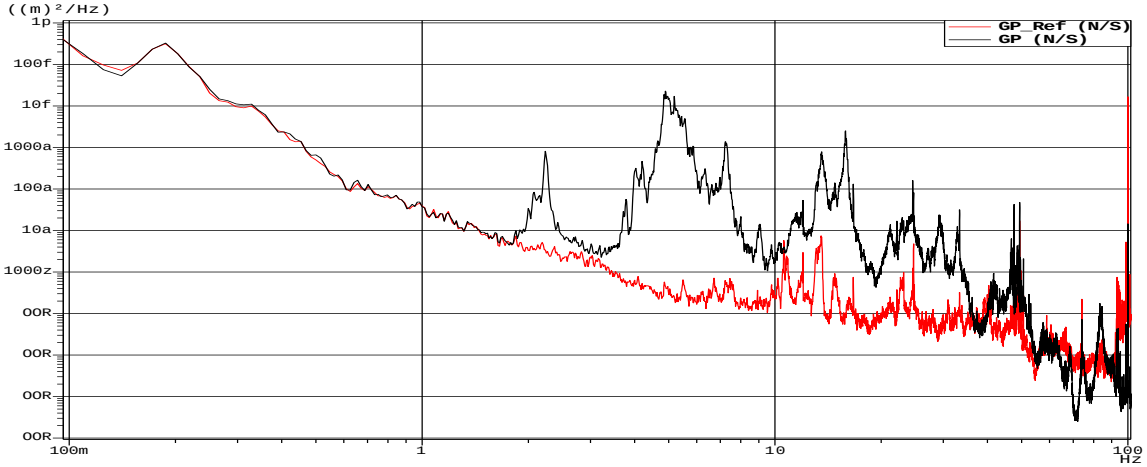

Figure F2. PSD of the signal North-South (Beam) direction.

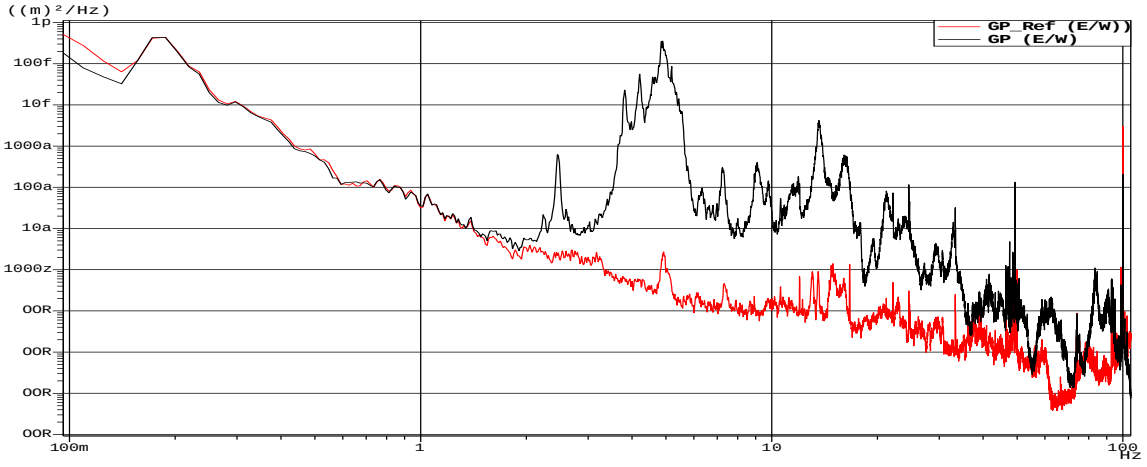

Figure F3. PSD of the signal East-West (Transversal) direction.

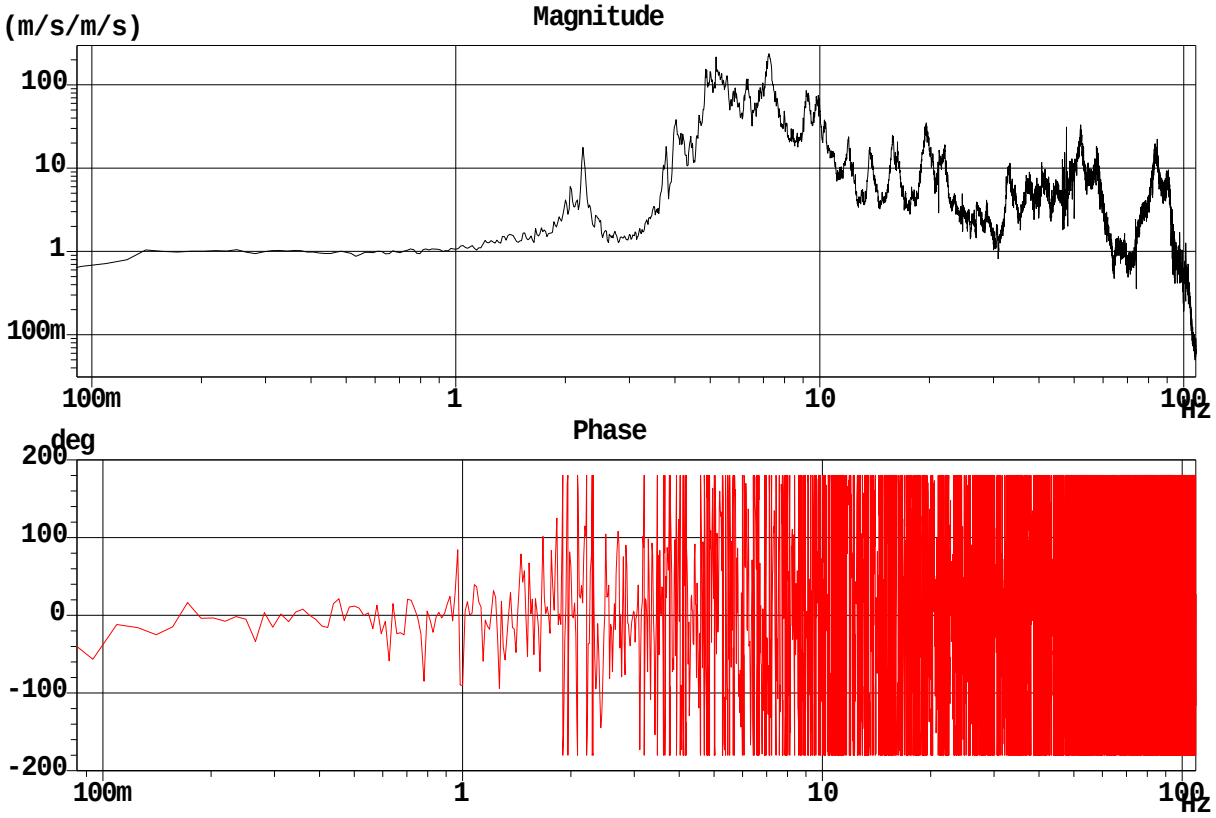

Figure F4: Transfer Function of the rotating shielding in the vertical direction

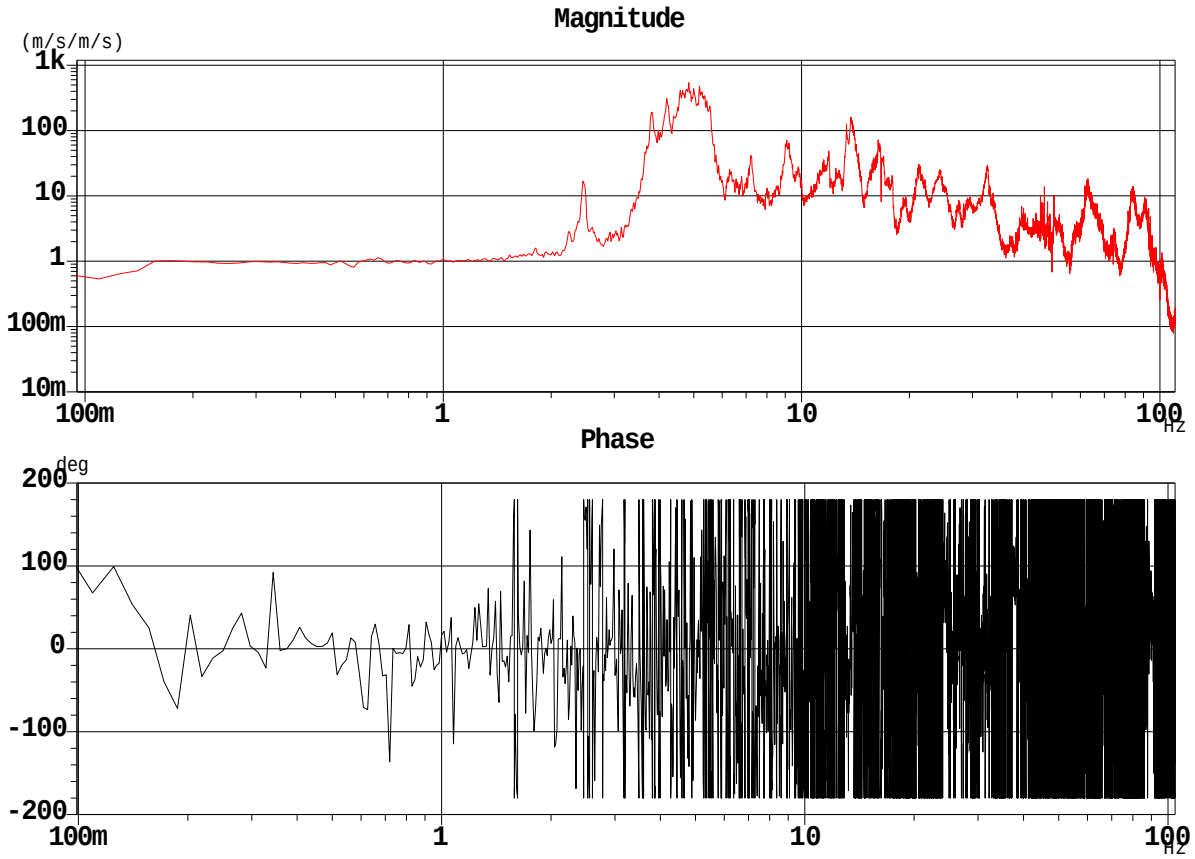

Figure F5: Transfer Function of the rotating shielding in the lateral direction